energies

MDPI

Article

Effect of Environmental Factors on Photovoltaic Soiling: Experimental and Statistical Analysis

Honey Brahma [1,*], Shraiya Pant [1], Leonardo Micheli [2,*], Greg P. Smestad [3] and Nabin Sarmah [1]

[1] Department of Energy, Tezpur University, Tezpur 784028, Assam, India
[2] Department of Astronautical, Electrical and Energy Engineering, Sapienza University of Rome, 00184 Rome, Italy
[3] Sol Ideas Technology Development, P.O. Box 5729, San José, CA 95150, USA
* Correspondence: honeybrahma325@gmail.com (H.B.); leonardo.micheli@uniroma1.it (L.M.)

Abstract: Soiling significantly impacts PV systems' performance, but this can be mitigated through optimized frequency and timing of cleaning. This experimental study focused on the conditions leading to soiling. It utilized a novel method to evaluate the effectiveness of different cleaning frequencies. The transmittance of horizontally mounted glass coupons exposed outdoors in a warm and humid location was measured weekly and these measurements were used (i) to evaluate the variability of soiling and its seasonal correlations with environmental factors using linear regression models and (ii) to assess the effectiveness of the different cleaning cycles using statistical (F- and *t*-test) analysis. The minimum transmittance loss occurred during the season with the most frequent rainfall, which acted as the dominant natural cleaning agent. The experimental campaign showed that rainfalls do not completely clean soiling; a minimum intensity threshold has to be achieved to have a cleaning effect. The threshold rainfall was the highest for the weekly cleaned glass coupon and lowest for a coupon that was never cleaned. Based on the statistical analysis, it is suggested that weekly cleanings during winter and post-monsoon seasons and monthly cleanings during pre-monsoon and southwest monsoon seasons are optimal for areas in the Köppen–Geiger Cwa climate classification category. The correlation between soiling and environmental parameters was found to be highly dependent on the season. It may therefore not be possible to develop a simple, universal predictive relationship for soiling losses. The presented methodology is applicable to additional locations, even outside of the study area of India, to contribute to the understanding and mitigation of soiling.

Keywords: soiling; photovoltaic; transmittance loss; environmental parameters; linear regression; statistical analysis

Citation: Brahma, H.; Pant, S.; Micheli, L.; Smestad, G.P.; Sarmah, N. Effect of Environmental Factors on Photovoltaic Soiling: Experimental and Statistical Analysis. *Energies* **2022**, *15*, 0. https://doi.org/

Academic Editors: Susana Fernández and Julio Cárabe

Received: 28 October 2022
Accepted: 9 December 2022
Published: 20 December 2022

1. Introduction

In 2018, renewable energy sources generated 25.4% of the electricity consumed worldwide [1]. Target 7.2 of the United Nations Sustainable Development Goals aims to further increase their share in the global energy mix by 2030. Solar photovoltaics (PV) is the third largest renewable source of electricity globally [1] with 758.9 GW total cumulative installed capacity in 2020 [2]. The performance of PV systems is affected by parameters such as irradiance, shading conditions [3], temperature, and additional conditions, such as soiling [4]. Soiling consists of dust deposition on the surface of PV modules and is a natural phenomenon due to local environmental and meteorological conditions, as well as each system's configuration and design. Studies have been carried out across the globe to understand the impact of soiling on PV technologies, either by considering glass samples (which can act as a proxy of the glass surface of a PV module) [5,6] or PV modules [7,8]. Al Shehri et al. [9] studied the effect of dust accumulation on the transmittance of glass by exposing glass samples to the outdoor environment in Thuwal, Saudi Arabia, for one week to obtain a maximum reduction of 2% on the first day compared to a clean glass sample.

Boyle et al. [10] observed a reduction in light transmission of 11% through the cover glass due to natural dust deposition while preventing natural cleaning by rainfall during 5 weeks in a rural and mixed industrial and residential area of Colorado, USA. Overall, soiling has been estimated to cause significant losses worldwide to photovoltaic [11], building-applied photovoltaic (BAPV) [12], and concentrating solar power (CSP) systems [13].

Because of its substantial impact on the energy and economics of the global energy scenario, soiling has received significant attention from the research and industrial communities [14]. Therefore, it is essential to understand and maintain high conversion efficiency of PV systems under varying environmental conditions [15]. There is a complex relationship between the environmental parameters and the soiling of a PV surface. Investigations on their impact on soiling were reported [16], and some investigations have examined the interdependency of environmental parameters on soiling [17]. It is important to highlight that the environmental parameters influencing soiling typically also have seasonal trends that are also reflected in the loss profile. These seasonal trends were studied in arid, dry, and dusty locations of the United Arab Emirates (UAE) [18] and Indonesia [19]. Recently, it was reported that in Qatar, the highest soiling deposition rates occur in the colder season, followed by summer [20]. They were lowest in the rainy season.

Ideally, if the correlations between soiling and the significant environmental parameters were known, these could be used to predict the soiling loss based on the environmental parameters of a location. A regression model is a useful statistical tool to explore the relationships between the independent variables (such as the environmental parameters) and the dependent variables (i.e., indices representing soiling loss). Regression models have been used to investigate the impact of rainfall and particulate matter (*PM*) concentration on the soiling ratio [21], *PM10*, relative humidity, and wind speed on deposition and removal rates [17] and on the clearness index [22]. All these studies assumed that immutable correlations would exist between soiling and environmental parameters. In reality, it is not possible to exclude the idea that the correlations could change throughout the year, as the dominant parameters and their magnitude change with the seasons. Therefore, this work aims to investigate this seasonal behavior, making use of data collected over a year-long experimental campaign conducted in a location characterized by markedly seasonal soiling, which leads to non-negligible losses on the yield of PV systems.

In contrast with many other reliability issues that can affect PV systems, soiling is fully reversible. This means that it can be removed through either natural or artificial cleanings. Recently it has been reported that anti-soiling coatings can be used as an efficient strategy for reducing the effect of soiling on the performance of PV modules [23]. Artificial cleanings are performed either manually or by employing robots, with associated monetary costs. Recently, a case study in a semi-arid location in Morocco reported 3 weeks of cleaning frequency to achieve high financial gain [24]. Therefore, optimizing the cleaning frequency is important in minimizing expenses and energy losses [25]. Cleaning optimization should not neglect the most common natural cleaning agent, rain, whose pattern is strongly seasonal. In addition, not all rainfall has a cleaning effect: in some cases, it has been reported that soiling might not be removed from low-intensity rain events [26]. A recent study [20] has proposed that the cleaning effect of rainfalls increases proportionally to their intensities, following a logistic fit.

Due to all these reasons, the present study aims at (i) proposing a novel model to evaluate the effectiveness of different cleaning cycles for various seasons, (ii) experimentally investigating the seasonal correlations between soiling and various environmental parameters, and (iii) determining the rainfall threshold required to clean the glass surface. The methodology and the structure of the present experimental work are summarized in Figure 1. Overall, this study addresses the need of the PV community for methods to better model and predict the soiling losses and to recommend adequate mitigation solutions based on the technical aspects. It also contributes to the study of the seasonality of soiling and provides novel information that can help improve its modeling. The study was conducted in a region of India that is humid and has a dry winter. In light of this, novel experimental

data presented in this work can significantly benefit the PV deployment and maintenance in the region and in additional locations which share similar weather conditions and seasonal patterns (which are many). Since the proposed methodology can be applied to any site, the work described here is not simply of regional importance.

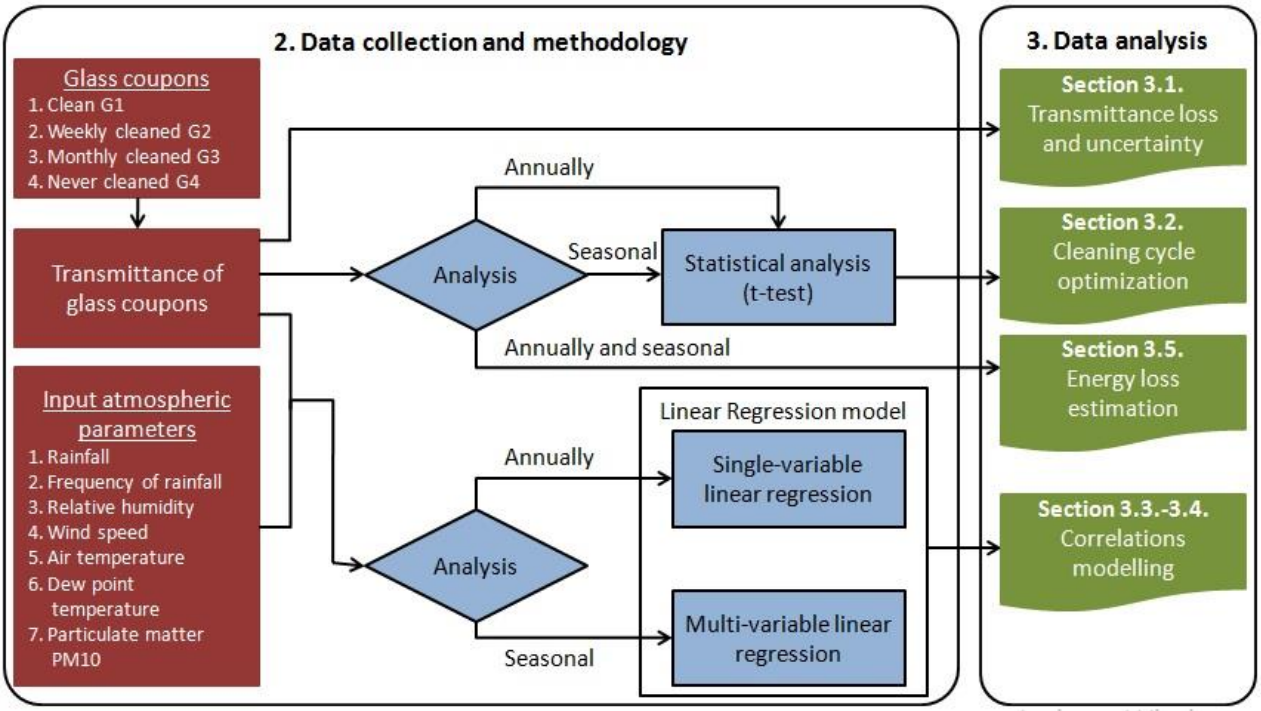

Figure 1. Flowchart of the novel methodology that can (i) evaluate the variability of soiling and its seasonal correlations with environmental factors using the linear regression models and (ii) assess the effectiveness of the different cleaning cycles using the statistical (F- and *t*-test analysis. The results are presented in the indicated sections.

2. Materials and Methods

2.1. Location Description

The methodology presented in this work was validated with outdoor data collected in Tezpur, Assam (latitude 26.62° N and longitude 92.79° E), on the northern bank of the river Brahmaputra in Northeast India. The location has a warm, humid, temperate climate with a dry winter and a hot summer; it falls under the Cwa category as per the Köppen–Geiger climate classification [27]. This designation applies to locations as diverse as Busan, South Korea; Lucknow, India; Zhengzhou, China; Hong Kong; Lilongwe, Malawi; Mackay, Queensland; Santiago del Estero, Argentina; and Guadalajara, Jalisco, Mexico. The experiments were conducted within the Tezpur University campus around 10 km from Tezpur. The characteristics of particles deposited due to soiling in Tezpur during a typical month, April, are given in Supplemental Materials' Table S1 and Figures S1 and S2.

This part of the country experiences four distinct seasons: winter (January and February), pre-monsoon (March to May), southwest (SW) monsoon (June to October), and post-monsoon (November and December) [28,29].

2.2. Environmental Parameters

The seasonal change in the environmental parameters that could be observed throughout the year is depicted in Figure 2 (also refer to the left side of Figure 1). The week number in this study starts from the week in which the experiment was initiated and it is not related to the week of the year. The environmental parameters such as rainfall intensity, wind speed, relative humidity, and ambient air temperature were measured at 1-minute intervals by a weather station (Station: Tezpur University, under the National Institute of Wind

Energy, India) installed near the experimental site. The values of environmental parameters in Figure 2, rainfall intensity, relative humidity (*RH*), wind speed (*Ws*), and air temperature (T_{amb}), are the weekly average of the data collected every minute. There are many ways to sum and analyze the basic mm/minute data for rain. The average weekly rainfall intensity (*Rain*) in Figure 2 is the direct average of rainfall in mm/minute registered over the week × 60 min × 24 h. The highest value for *Rain* occurred during the SW monsoon (19.7 mm/day), with pre-monsoon (13.0 mm/day), post-monsoon (3.0 mm/day), and winter (1.9 mm/day) being the lowest. The maximum hourly rainfall intensity (R_{max}) is the maximum of the cumulative rainfall over an hour. The rainfall value recorded in mm/minute was summed for each hour of the week and the maximum value among them is the maximum weekly rainfall. The frequency of rainfall is denoted by R_f, which is the number of days with rainfall each week. The R_f fluctuates between 0 and 7 days per week during the SW monsoon while there are just 0 to 3 days per week during the winter. In winter, an extended dry period of up to 28 days has been recorded (i.e., the weeks between 35 and 38). R_f is extremely high during SW monsoon, gradually falls during the post-monsoon and winter, then rises again during pre-monsoon; this cycle is typical for the area under study. Weekly mean particulate matter concentrations were obtained from the Pollution Control Board, Department of Environment and Forest, Government of Assam (Station: Tezpur- 536). The average weekly particulate matter (*PM10*) is the direct average over the week. The *PM10* concentration recorded was 135 μg/m^3 during winter and 128.5 μg/m^3, 107.8 μg/m^3, and 95.3 μg/m^3 during post-monsoon, pre-monsoon, and SW monsoon, respectively. The *RH* for a year lies in the range of 70–98%, depending on the intensity and frequency of the rainfall. It is relatively low during the winter (84.4%) and during the SW monsoon, it is at its maximum (93.2%). The average weekly air temperature (T_{amb}) during the SW monsoon and pre-monsoon is high, ranging from 9 °C to 21 °C, whereas the T_{amb} gradually decreases from post-monsoon to winter in the range of 6 °C to 13 °C.

The dew formation on the PV surface is one of the parameters that can influence soiling [30]. Dew point temperature is dependent on the *RH* and T_{amb} and was calculated using the August–Roche–Magnus equation [31]:

$$\gamma = \ln\left(\frac{RH}{100}\right) + \frac{bT_{amb}}{d + T_{amb}} \quad (1)$$

where b = 17.67 and d = 243.5 °C. The dew point temperature is given by:

$$T_d = \frac{d\gamma}{b - \gamma} \quad (2)$$

The average weekly dew point temperature (T_d) during the SW monsoon, post-monsoon, winter, and pre-monsoon seasons are 16.7 °C, 8.1 °C, 4.9 °C, and 11.2 °C, respectively.

Higher wind speed values have been observed during the pre-monsoon season with maximum instantaneous wind speed values up to 12 m/s, resulting in a 2.2 m/s weekly average wind speed (*Ws*) during the season. The maximum percentage of the wind (22.8%) within the range of 2–4 m/s irrespective of direction is also experienced in this season, one that has a higher tendency of depositing dust onto a surface [32]. *Ws* higher than 6 m/s was extremely rare, i.e., <0.1% of the occurrences in all the seasons. For the total percentage contribution for different ranges of *Ws*, summed from all directions during the various seasons, see Table S2 and Figure S3.

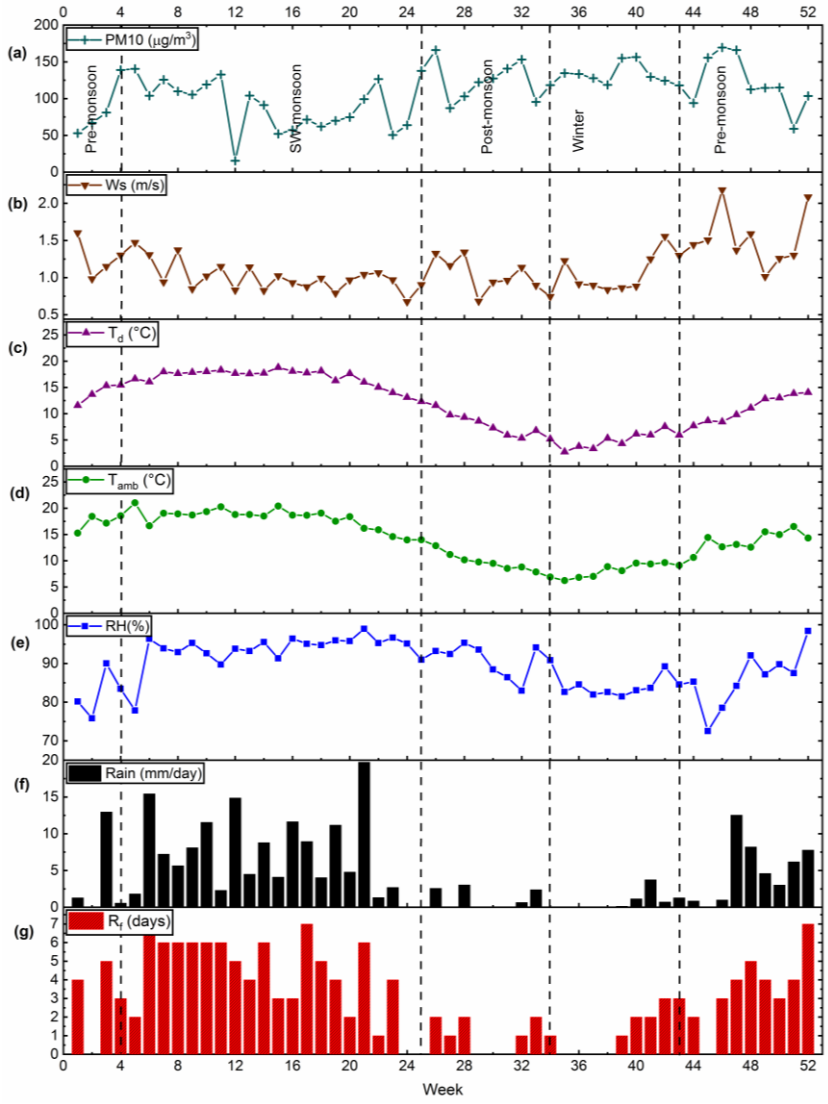

Figure 2. The average weekly value of the environmental parameters (**a**) particulate matter, *PM10* (μg/m^3); (**b**) wind speed, *Ws* (m/s); (**c**) dew point temperature, T_d (°C); (**d**) ambient air temperature, T_{amb} (°C); (**e**) relative humidity, *RH* (%); (**f**) rainfall intensity, *Rain* (mm/day), which is equal to the direct average, over a given week, of the rainfall recorded in mm per minute multiplied by 60 min × 24 h; and (**g**) weekly frequency of rainfall R_f (days).

2.3. Measurement of Transmittance

Four low iron glass coupons of dimension 4 cm × 4 cm with 3 mm thickness were mounted horizontally in an open rack at a 1.5 m height (Figure 3). The use of a horizontal orientation for glass coupons is standard practice in the study of soiling and was employed in our previous study, which compared soiling at several sites worldwide [33]. Horizontal orientation can allow for more facile and direct comparisons across different sites and often provides the maximum possible rate of soiling for the fundamental studies that are the focus of this work. The deposition velocity utilized in the first principle (ab initio) soiling models is parallel to the force of gravity and normal to the horizontal plane [13]. In addition, solar panels installed on many flat roofs for commercial systems are tilted at less than 5° to maximize power density per unit area and minimize shading losses between the rows.

In this work, glass coupons are used in place of PV modules. This approach has been frequently used as a standard method in PV soiling studies, as it makes it possible to characterize the accumulated particles more. In 2015, Burton et al. [34] employed indoor

and outdoor mounted coupons to investigate the correlation between the mass density of soiling and the transmittance loss. Boyle et al. [35] used the same outdoor setup deployed in two sites to study the correlation between suspended and deposited particulate matter. Conceição et al. [36] measured the dust accumulated on glass coupons every week to evaluate the impact of Saharan desert dust storms in Portugal. Nayshevsky et al. [37] investigated the effectiveness of hydrophobic-hydrophilic coatings in facilitating dew collection and, therefore, natural cleanings using glass coupons. It should be noted that coupons are nowadays used not only for research purposes but also in commercial soiling sensors. DustIQ, a sensor developed by Kipp & Zonen, estimates soiling by measuring the reflectance of soiling accumulated on its front glass. A first validation was presented by Korevaar et al. [38], who compared the DustIQ measurements with those of a soiling station in Morocco. The Mars optical sensor, developed by Atonometrics, estimates soiling by determining the transmittance loss that occurred through its front glass. A team from QEERI [39] found a strong correlation between the losses measured by Mars and estimated from a PV array in Qatar. The glass coupons were numbered as follows: G1 (reference glass, kept clean inside a sealed box), G2 (cleaned weekly), G3 (cleaned monthly), and G4 (never cleaned). The cleaning cycles (or frequencies) were chosen arbitrarily and for illustrative purposes to capture the different magnitudes of time scales for possible cleaning frequencies in actual PV power plants. Cleanings were performed using water and a microfiber cloth. The coupons were exposed to outdoor conditions from May 2018 to May 2019. The direct spectral transmittance of these glass coupons was measured weekly in the 350–1000 nm wavelength range with a 1 nm increment using a UV-Vis spectrophotometer (UV-10).

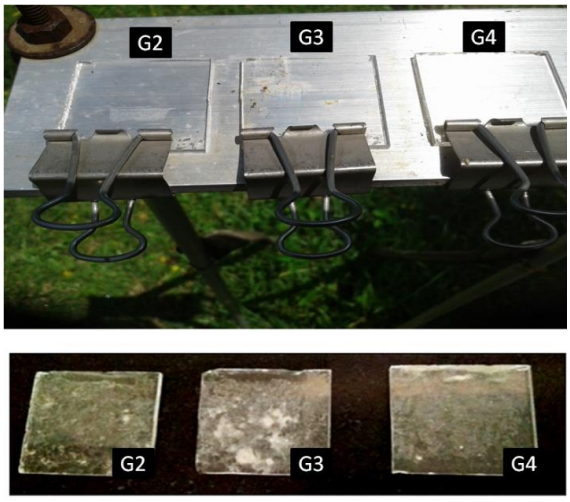

Figure 3. Photographs of the glass coupons placed outdoors having different cleaning cycles, weekly cleaned (G2), monthly cleaned (G3), and never cleaned (G4) (**above**), and an example of the non-uniform distribution of soiling observed, for example, at week 45 (**below**).

The measured direct transmittance of each glass coupon was normalized to the direct transmittance of the clean glass [33]. In this way, the impact of the transmittance of the glass was eliminated. The relative direct spectral transmittance $\tau_r(\lambda)$ is expressed as:

$$\tau_r(\lambda) = \frac{\tau_{soiled}(\lambda)}{\tau_{clean}(\lambda)} \quad (3)$$

where $\tau_{soiled}(\lambda)$ and $\tau_{clean}(\lambda)$ are the measured direct spectral transmittance of the soiled and clean glass coupons, respectively. As one of several quality checks for the transmittance data, the weekly τ_r versus wavelength was checked against the modified Ångström turbidity equation (Equation (S1)) from an earlier publication [33]; a few examples are shown in

Figures S4 and S5. The soiling transmittance loss of exposure was calculated for each week as [33]:

$$\tau_{loss} = (1 - \tau_r) \quad (4)$$

The average relative direct transmittance, τ_r, is the simple average over the wavelength range 350–1000 nm of the spectral transmittance averaged using three spots on the glass coupon. The broadband direct spectral transmittance of the clean glass is 0.91. This work uses τ_r and τ_{loss} of soiled glass to investigate cleaning strategies and the correlation between the transmittance due to soiling and several key environmental parameters.

Depending on the incident solar irradiance and the PV technology, their power output changes with soiling. This can be estimated given the experiments conducted and the resulting measurements. The energy yield loss from a PV panel due to soiling is calculated as:

$$E_{loss} = E_{clean} - E_{soiled} \quad (5)$$

where E_{clean} is the energy yield from a PV panel with no soiling and E_{soiled} is the energy yield from a PV panel with soiling. Equation (5) is analogous to Equation (4). Further,

$$E_{clean} = P_{clean}\ H_s \quad (6)$$

$$E_{soiled} = P_{soiled}\ H_s \quad (7)$$

where P is the power output and subscripts clean and soiled are for PV modules with no soiling and with soiling, respectively. H_s is the number of sunshine hours. The location of the study site has on average 9 sunshine hours in the pre-monsoon and SW monsoon seasons, and 8 h for the post-monsoon and winter seasons [40]. The power output is expressed as:

$$P = J_{sc}\ r_s\ V_{oc}\ FF \quad (8)$$

where J_{sc} is the short-circuit current density, V_{oc} is the open-circuit voltage, and FF is the fill factor. Here, r_s is 1 for a clean PV module and decreases while the losses increase (in Equation (8)). Indeed, the soiling loss (power loss due to soiling) can be calculated as $(1 - r_s)$, where r_s is the soiling ratio, as defined in [41,42]. Under the assumption of uniformly distributed soiling, the instantaneous soiling ratio at a time t can be expressed as:

$$r_s(t) = \frac{J_{sc\_soiled}(t)}{J_{sc\_clean}(t)} \quad (9)$$

where $J_{sc\_soiled}(t)$ is the short-circuit current density of the module under natural soiling and $J_{sc\_clean}(t)$ is the short-circuit current density of the clean module. Equation (9) can also be expressed as:

$$r_s(t) = \frac{J_{sc\_soiled}(t)}{J_{sc\_clean}(t)} = \frac{\int_{\lambda_2}^{\lambda_1} E_D(\lambda,t)\ \tau_r(\lambda,t)\ SR(\lambda) d\lambda}{\int_{\lambda_2}^{\lambda_1} E_D(\lambda,t)\ SR(\lambda) d\lambda} \quad (10)$$

where λ_1 and λ_2 are the upper and lower limit of the absorption band of the PV material, respectively. $E_D(\lambda,t)$ is the direct spectral distribution of the solar irradiance as defined by the ASTM G173-03 Standard [43]. $SR(\lambda)$ is the spectral response of the PV material. Here, the spectral response of a monocrystalline silicon solar cell of the Saturn series from BP Solar was utilized (Figure S9). Equations (9) and (10) can be compared to Equation (3) to justify the utilization of relative transmittance in this study.

2.4. Linear Regression Model

Both the single-variable linear regression (SLR) and multi-variable linear regression (MLR) models have been used to correlate the environmental parameters to the transmittance of the glass coupon. In this model, the dependence of the transmittance of the glass

coupon on the considered (individual) environmental parameters was investigated. The Microsoft Excel regression analysis tool was used for linear curve fitting. The transmittance of the glass coupon is considered a linear function of the environmental parameter(s) and is expressed as:

$$\tau_r = \alpha_0 + \alpha v \tag{11}$$

where α_0 is the intercept, v is the environmental parameter's value, and α is its coefficient. Similarly, MLR is expressed as:

$$\tau_r = \alpha_0 + \alpha_1 v_1 + \alpha_2 v_2 + \alpha_3 v_3 + \ldots + \alpha_n v_n \tag{12}$$

where α_0, α_1, α_2, α_3, . . . , α_n are the intercept and the variables' coefficients and v_1, v_2, v_3, . . . , v_n are the input environmental parameters.

The p-value and R^2 are used to quantify the quality of the regression. The p-value describes the significance of the relationship and the R^2 value indicates the degree to which the dependent variable is explained by the model [44]. The input parameters of the correlation are considered significant if the p-value < 0.05. The model used combinations of the environmental parameters to estimate the weekly transmittance of glass coupon G2 (cleaned weekly).

2.5. Statistical Analysis

The statistical F-test and t-test should be carried out to determine the statistically meaningful differences in net soiling on a seasonal basis. These tests are based on hypothetical assumptions: the F-test null hypothesis states that the two samples have the same variance and the t-test null hypothesis states that the difference between the means of the two samples is equal. The null hypothesis for the F- or t-test cannot be rejected when the absolute F- or t-statistic is less than the absolute F- or t-critical two-tail value and the p-value is greater than 0.05. Initially, the F-test analysis was analyzed to determine the equality or inequality of the variance of two samples. Following that, a t-test with equal variance was performed if the p-value > 0.05, and a t-test with unequal variance analysis was been performed if the p-value < 0.05.

The statistical errors provide the accuracy level of the predicted data from the model [45], such errors as the mean squared error, MSE in Equation (S4), and the root-mean-square error, RMSE in Equation (S5). Here, these errors were calculated between the predicted and measured average relative direct transmittance of the glass coupon, G2. These predicted values were obtained while correlating the measured relative direct transmittance and the various environmental parameters for various seasons.

3. Results

3.1. Transmittance Loss

Figure 4 shows the drop in the weekly τ_r of the glass coupons G2, G3, and G4 relative to G1 (clean glass), and also the total rain intensity during the week. The transmittance losses (calculated using Equation (4)) due to soiling in the various seasons can be ranked in this order: winter > post-monsoon > pre-monsoon > SW monsoon. The maximum average transmittance loss (τ_{loss}) was 24.4% for G4 (never cleaned), 18.4% for G3 (monthly cleaned), and 16.6% for G2 (weekly cleaned), all of which were recorded during the winter season. Our method utilizes a frequency distribution plot as shown in Figure 5 to aggregate and analyze the data in Figure 4 for each of the three cleaning cycles. A glass coupon when cleaned weekly maintains a high frequency of τ_r values above 96%, as opposed to the never cleaned coupon for which the τ_r can decrease to 63.6% over the year (Figure 5). Based on the cleaning cycle, the maximum decrease was found for G4, followed by G3 and G2. The seasonal and annual average τ_{loss}, uncertainty, and standard deviation of all the glass coupons are listed in Table 1 (For the standard deviation and uncertainty calculation, refer to Equations (S2) and (S3)). This forms the input shown in the top and middle boxes at the left in Figure 1. To understand the seasonal net soiling given the

high uncertainty and variability in the data, a statistical *t*-test analysis was performed. This will be described in the next section.

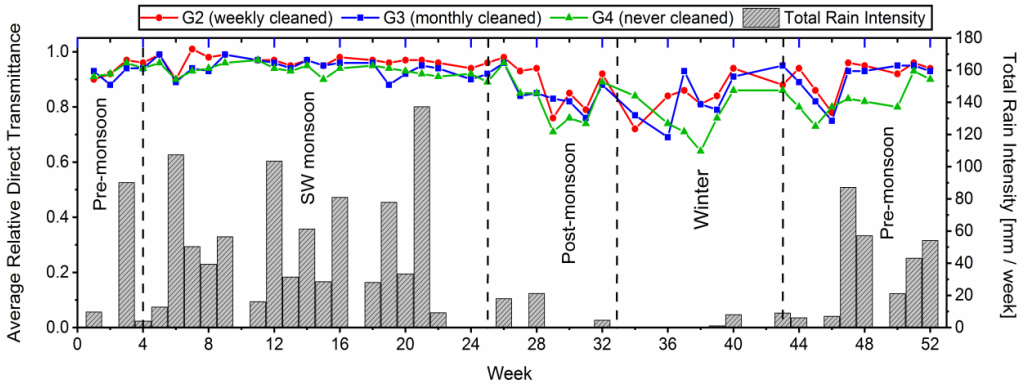

Figure 4. The average relative direct transmittance of glass coupons with different cleaning cycles (G2, G3, and G4) and total rainfall intensity (in mm/week) in consecutive weeks of the year.

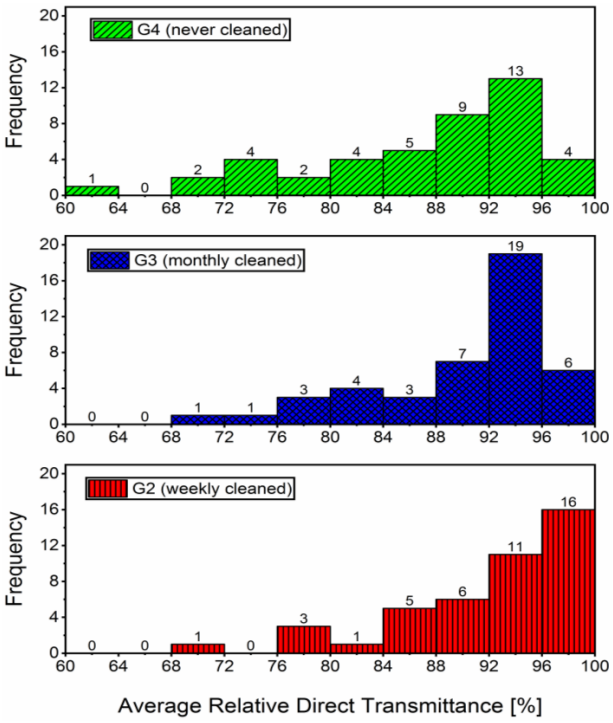

Figure 5. Frequency distribution of the average relative direct transmittance of the weekly cleaned (G2), monthly cleaned (G3), and never cleaned (G4) glass coupons over the year.

Table 1. The seasonal and annual average (Avg) transmittance loss (τ_{loss} in %), seasonal average uncertainty (%), and seasonal average standard deviation (SD in %) in the average relative direct transmittance (τ_r) of different glass coupons. The average relative direct transmittance is the average for measurements taken at three spots of the glass coupon over the wavelength 350-1000 nm.

Season	G2			G3			G4		
	Avg [%]	Uncertainty [%]	SD [%]	Avg [%]	Uncertainty [%]	SD [%]	Avg [%]	Uncertainty [%]	SD [%]
Pre-monsoon	8.5	±1.8	±5.3	9.6	±1.9	±6.2	14.5	±2.7	±6.9
SW monsoon	3.4	±0.9	±2.2	5.8	±0.9	±3.1	6.6	±0.8	±2.3
Post-monsoon	11.9	±2.2	±8.3	15.1	±2.3	±6.2	17.5	±3.4	±8.8
Winter	16.6	±3.1	±7.2	18.4	±3.3	±9.1	24.4	±0.7	±8.3
Annually	7.9	±2.0	±5.8	10	±2.1	±6.1	13	±1.9	±6.6

3.2. Statistical F-Test and t-Test Analysis

For the site under study, where the method was tested, the seasonal F- and *t*-test statistical analysis for combinations of cleaning cycles are shown in Table 2. It was observed that there was no statistical difference in the net soiling when the glass coupons were either monthly or never cleaned irrespective of whether it was analyzed on a seasonal basis or annual basis. During the SW monsoon season, the statistical difference in net soiling could be seen when the glass coupon was cleaned weekly or left uncleaned. However, the difference was insignificant for other seasons. The net soiling during winter and post-monsoon seasons were statistically the same irrespective of different cleaning cycles. A week-long exposure during post-monsoon and winter can decrease the transmittance of glass coupons to values as low as those for a coupon that is never cleaned. Therefore, frequent cleaning (once a week) during post-monsoon and winter seasons is recommended to maintain high transmittance. However, cleaning once a month during pre-monsoon and SW monsoon season is found to be enough to maintain high transmittance, because a week of exposure does not reduce the transmittance of glass coupons by much when compared to a month's exposure or when the coupon is never cleaned.

Table 2. The F-test and *t*-test statistical analysis comparing the weekly cleaned (G2), monthly cleaned (G3), and never cleaned (G4) glass coupons. This represents the topmost rectangle for the data collection and methodology section in the flowchart of Figure 1.

Season	**Combination of Glass Coupons**					
	G2–G3		**G2–G4**		**G3–G4**	
	F-Test	***t*-Test**	**F-Test**	***t*-Test**	**F-Test**	***t*-Test**
Pre-monsoon	x	x	x	✓	x	x
SW monsoon	x	✓	x	✓	x	x
Post-monsoon	x	x	x	x	x	x
Winter	x	x	x	x	x	x
1 Year	x	x	x	✓	x	x
Non-monsoon	x	x	x	✓	x	x
High-soiling	x	x	x	✓	x	x
Low-soiling	x	✓	✓	✓	✓	x

✓: F/*t*-test null hypothesis is rejected (significant difference in the variance/means). x: F/*t*-test null hypothesis cannot be rejected (no significant difference in the variance/means). Non-monsoon season includes winter, pre-monsoon, and post-monsoon seasons. High-soiling season includes week 24 until week 46. Low-soiling season includes weeks 1–23 and weeks 47–52. The low-soiling and high-soiling seasons are classified based on the rainfall intensity received. The weeks with high rainfall are in the low-soiling season and weeks with low or no rainfall are in the high-soiling season.

The F- and *t*-test statistical analysis for all cleaning cycles showed that both winter and post-monsoon seasons have a significant difference in net soiling compared to the SW monsoon season. However, the difference is insignificant between winter and post-monsoon seasons and between post-monsoon and pre-monsoon seasons. Weekly cleaning and no cleaning during the pre-monsoon and SW monsoon seasons showed clear differences in the mean values, whereas monthly cleaning showed no significant difference in their mean values. (For the *t*-test analysis between different seasons for different cleaning cycles, see Figure S6.) Therefore, the seasons are divided into two categories: monsoon (SW monsoon) versus non-monsoon (includes post-monsoon, winter, and pre-monsoon) and low-soiling versus high-soiling seasons to analyze the difference between the cleaning cycles. As shown in Figure 6, weekly cleaned and never cleaned glass coupons are statistically different. Similar statistical results were observed during the low-soiling and high-soiling seasons, as is summarized in Figure 7. These results are also summarized in Table 2. Had this statistical approach not been employed, erroneous conclusions might have been made,

and conclusions that are on more solid footing might have been overlooked. This highlights one strength of our methodology (see Figure 1).

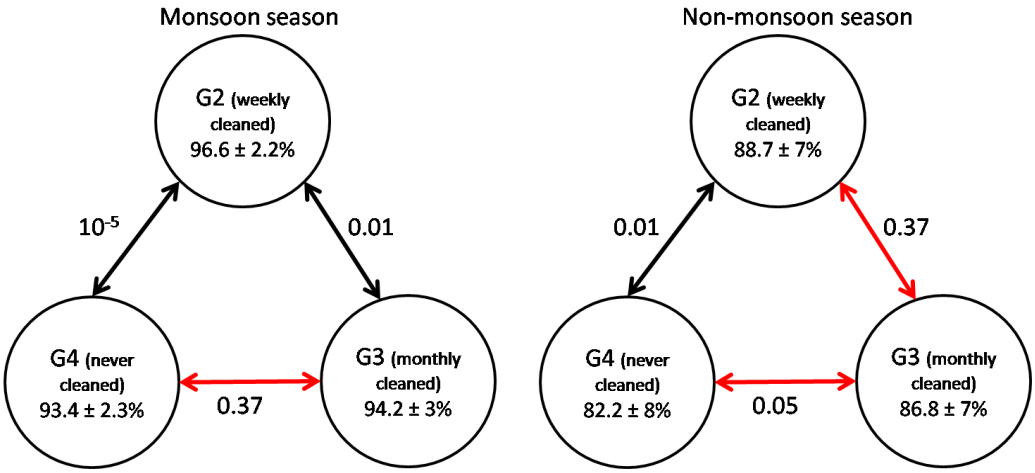

Figure 6. The *t*-test analysis between different cleaning cycles: weekly cleaned (G2), monthly cleaned (G3), and never cleaned (G4) glass coupons for the monsoon (**left**) and non-monsoon (**right**) seasons. The *p*-value is given, as well as the average and standard deviation (refer to Table 1).

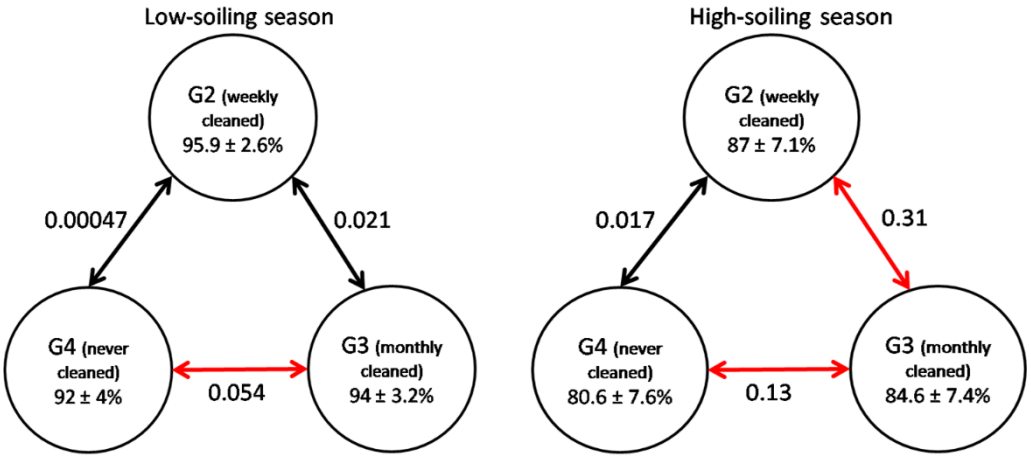

Figure 7. The *t*-test analysis between different cleaning cycles: weekly cleaned (G2), monthly cleaned (G3), and never cleaned (G4) glass coupons for the low-soiling (**left**) and high-soiling (**right**) seasons. The *p*-value is given, as well as the average and standard deviation (refer to Table 1).

3.3. Correlation between the Transmittance and the Environmental Parameters

The effect of the environmental parameters on the τ_r value of the glass coupons has been analyzed to understand the impact of these environmental parameters on PV soiling at the location under study. This part of the recommended methodology is outlined in the bottom half of the flowchart given in Figure 1. The individual effect of each environmental parameter on the τ_r value of the glass coupons exposed to natural soiling has been analyzed using data from the whole year of exposure. Figure 8a–c show the correlation between the τ_r value for the G2, G3, and G4 glass coupons, respectively, and the maximum hourly rainfall intensity for each week (R_{max}). Following the previous finding of a study conducted in Qatar by Javed et al. [20], a nonlinear function of the logistic type was modeled to fit the correlation between average weekly τ_r and R_{max}. However, the correlation did not achieve high R^2 values (0.42 for G2, 0.40 for G3, and 0.39 for G4), attributed to the simultaneous effect of other environmental parameters on soiling. The winter season being 'dry' and hardly receiving any rainfall shows the lowest R_f compared to other seasons. As shown in Figure 8d, it could be observed that the slope of the logistic fit in the case of G2 and G3 is

not as steep as in G4. Moreover, the maximum limit of τ_r is highest for G2, followed by G3 and G4. The threshold rainfall was calculated from the logistic fit of the transmittance of a glass coupon versus the maximum rainfall (Figure 8a–c). The threshold value is the maximum rainfall at 95% of the limit of τ_r and was found to be 2.1 mm/h, 3.1 mm/h, and 3.4 mm/h for G4, G3, and G2, respectively. There exists a minimum threshold, and it depends on the cleaning strategy. The results suggest that the loose dirt is knocked off the glass surface with even less rainfall. In addition, even with the hardest rainfall, we do not achieve a relative transmittance for a never cleaned coupon equal to that of weekly or monthly cleaned coupons. This is a general conclusion that can be applied to other locations and other cleaning frequencies.

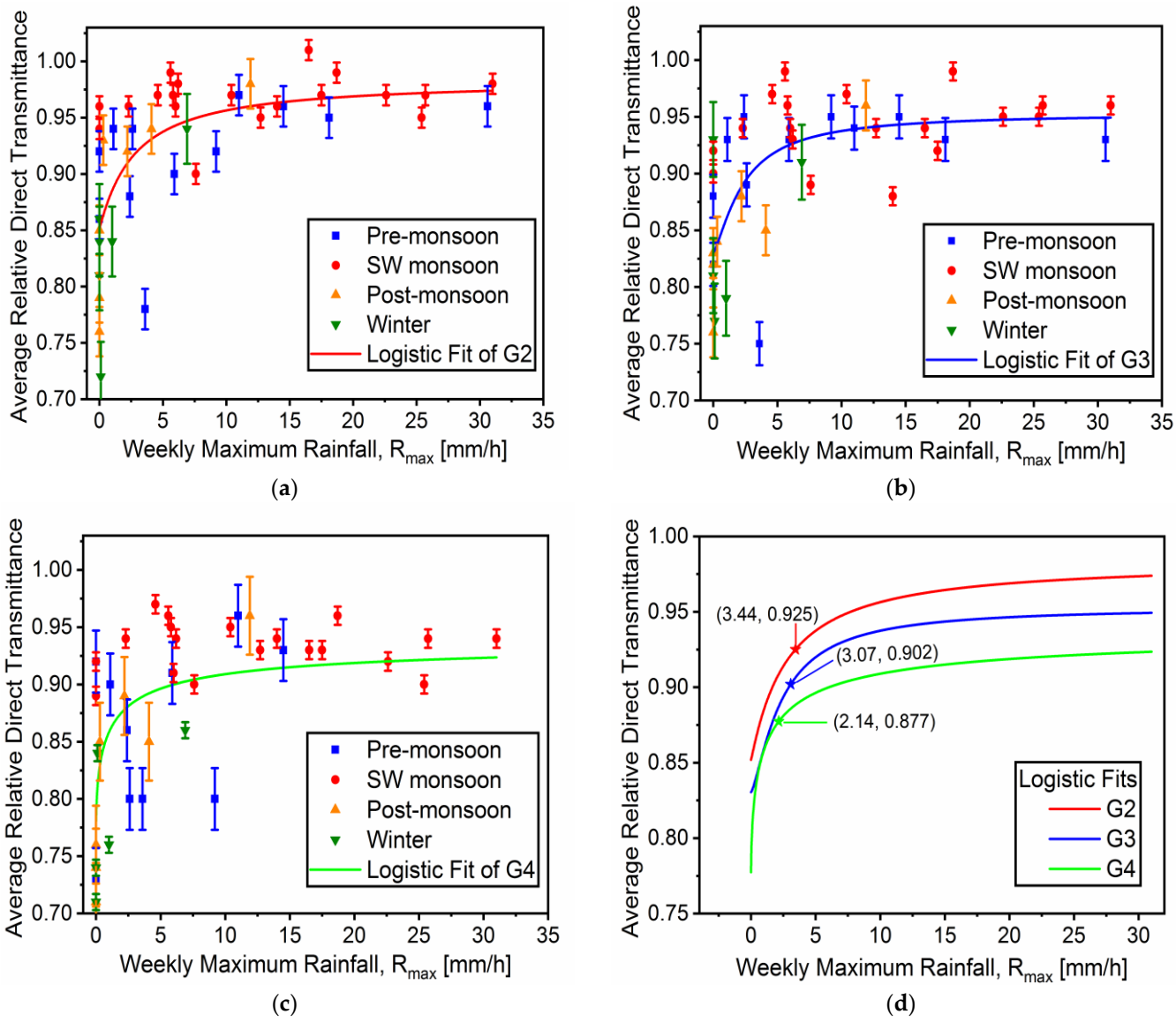

Figure 8. The average relative direct transmittance versus the weekly maximum rainfall (R_{max}) for the (**a**) weekly cleaned glass (G2), R^2 = 0.42; (**b**) monthly cleaned glass (G3), R^2 = 0.40; (**c**) never cleaned glass (G4), R^2 = 0.39; and (**d**) the threshold rainfall required to clean the glass coupon under various cleaning schedule. (The values of the parameters are provided in Table S3.)

The location of this study has remarkably high *RH*; always >70% throughout the year, which may lead to increased soiling. Previous studies [31,46] reported that for *RH* > 80% the dust particle removal rate is low because of the water capillary bridges formed between the particles and the glass surface due to the presence of condensed water. While the impact

of *RH* on soiling may be significant at the location under study, another factor defining the severity of soiling is the *PM10* concentration in the atmosphere. At the investigated site, where *RH* ranged between 72–98%, having a *PM10* < 80 μg/m^3 resulted in no significant soiling. For *PM10* in the range 80–120 μg/m^3, maximum τ_{loss} was observed for all the glass coupons. For *PM10* values above 120 μg/m^3, the severity of soiling increases when the glass coupons are never cleaned, as shown in Figure 9. (The plots for the weekly and monthly cleaned glass coupons are provided in Figure S7.) A year-long analysis showed no significant correlation between τ_r and *RH* and *PM10* simultaneously.

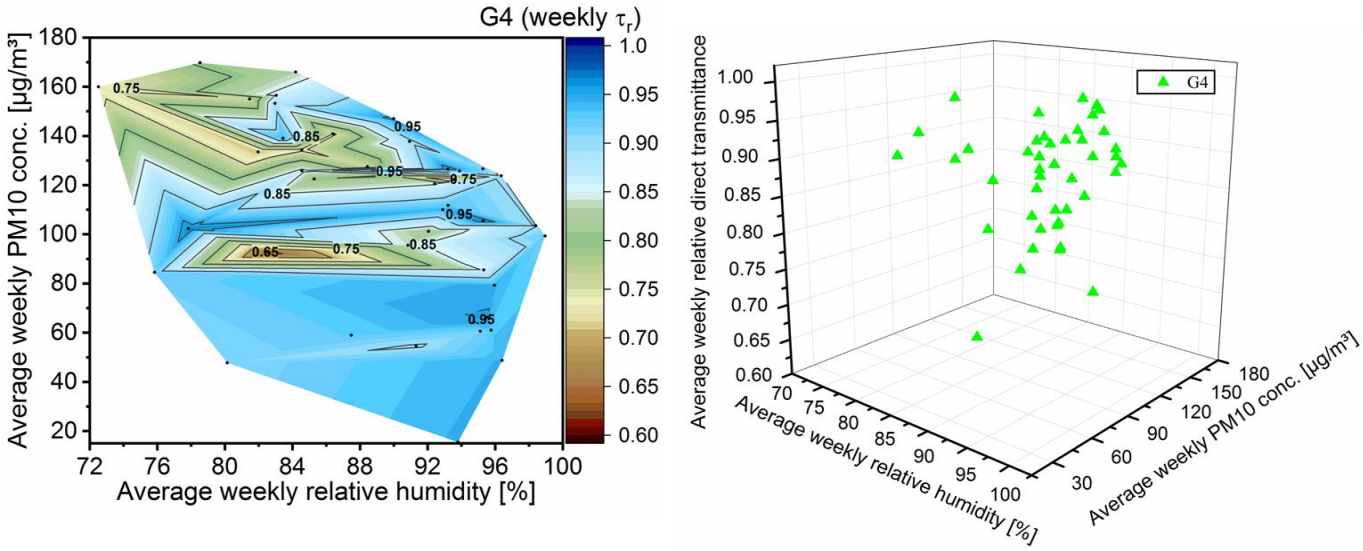

Figure 9. Correlation between the average relative direct transmittance (τ_r), the average weekly *PM10*, and relative humidity (*RH*) for the never cleaned (G4) glass coupon. The figure on the **right** shows the scatter plot for data on the **left**.

Another parameter influencing soiling that is related to *RH* is dew formation, which is a result of condensation. (For the correlation of τ_r with T_{amb} and T_d, see Tables S4 and S5.) Dew forms on a surface having a temperature lower than that of the atmosphere, especially during the night with a clear sky having suitable conditions for radiative cooling [30,31]. Over the year, the experiment recorded the average weekly ΔT < 6 °C, suggesting that dew can occur frequently at the site. The average weekly ΔT is the difference between the average weekly ambient air temperature, T_{amb}, and average weekly dew point temperature, T_d. (For the impact of ΔT and *PM10* on τ_r for the glass coupon G2, see Figure S8a.) The interplay between ΔT, *PM10*, and τ_r was found to be similar to that of between the *RH*, *PM10*, and τ_r. It was observed empirically that condensation occurred on glass surfaces while the combined conditions such as high *RH* and $T_d \geq (T_{amb} - 2.5\ ^\circ\text{C})$ were met (For details, see Figure S8b.). This is given by the number of hours in a week. It was observed that all the days of the week met the condition at least for a few hours. This was taken into consideration to explore the process of dew formation which could increase soiling by various mechanisms such as particle adhesion, cementation, and particle caking [30].

The yearly analysis carried out using the SLR model showed $p < 0.05$ but with a very low R^2 value for the correlation between τ_r for different glass coupons and the individual environmental parameters (Table S6). However, the R^2 value was very low, signifying poor correlation. Therefore, the MLR method was utilized to analyze the combined impact of different environmental parameters on a seasonal and yearly basis on the average relative transmittance (τ_r) of the weekly cleaned (G2) glass coupon, which is presented in the next section. The analysis for the monthly cleaned (G3) and never cleaned (G4) glass coupons are not analyzed in this way because the statistical *t*-test analysis showed that there existed no statistically significant difference in the mean of the τ_r of different cleaning cycles on seasonal basis except for the SW monsoon season.

3.4. Seasonal Analysis Using Multi-Variable Linear Regression (MLR)

Previous studies revealed the combined effect of *PM10* and R_f [47], rainfall and *Ws* [48], and *Ws* and *RH* [22] to significantly affect soiling at the investigated locations. In this work, the significant correlation between the τ_r and various environmental parameters determined seasonally and annually is presented in Table 3. (For orientation, refer to the lower right side of Figure 1.) Based on the relation obtained between the input environmental parameters and the τ_r for different seasons of the year, the predicted and measured datasets were plotted to obtain a linear relation using the linear regression method as shown in Figures 10–12 (for the correlation values obtained between the predicted and measured τ_r, see Table S7) and the statistical errors such as mean square error (MSE) and root-mean-square error (RMSE) were calculated using Equations (13) and (14) and are listed in Table 3.

Table 3. The seasonal analysis result of the MLR model in correlating the average relative direct transmittance of the weekly cleaned glass (G2) and the environmental parameters with a *p*-value < 0.05 along with the statistical errors mean square error (MSE) and root mean square error (RMSE) between the predicted and measured average relative direct transmittance.

Season	Input Environmental Parameters	MSE (%)	RMSE (%)	R^2	Standard Error	Relation
Pre-monsoon	R_f and *Ws*	0.08	2.78	0.70	0.03	$\tau_r = 0.019\ R_f - 0.12\ Ws + 1.02$
	Rain and *PM10*	0.08	2.90	0.67	0.03	$\tau_r = 0.0085\ Rain - 0.00066\ PM10 + 0.95$
Post-monsoon	R_f	0.11	3.31	0.81	0.04	$\tau_r = 0.083\ R_f + 0.81$
	Ws	0.07	2.66	0.88	0.03	$\tau_r = 0.33\ Ws + 0.53$
Winter	*Rain* and *Ws*	0.01	1.17	0.97	0.02	$\tau_r = 0.087\ Rain + 0.82\ Ws + 0.11$
	R_{max} and *Ws*	0.01	1.15	0.97	0.02	$\tau_r = 0.015\ R_{max} + 0.82\ Ws + 0.11$
1-year	R_f and T_{amb}	0.22	4.63	0.53	0.05	$\tau_r = 0.0043\ R_f + 0.010\ T_{amb} + 0.76$

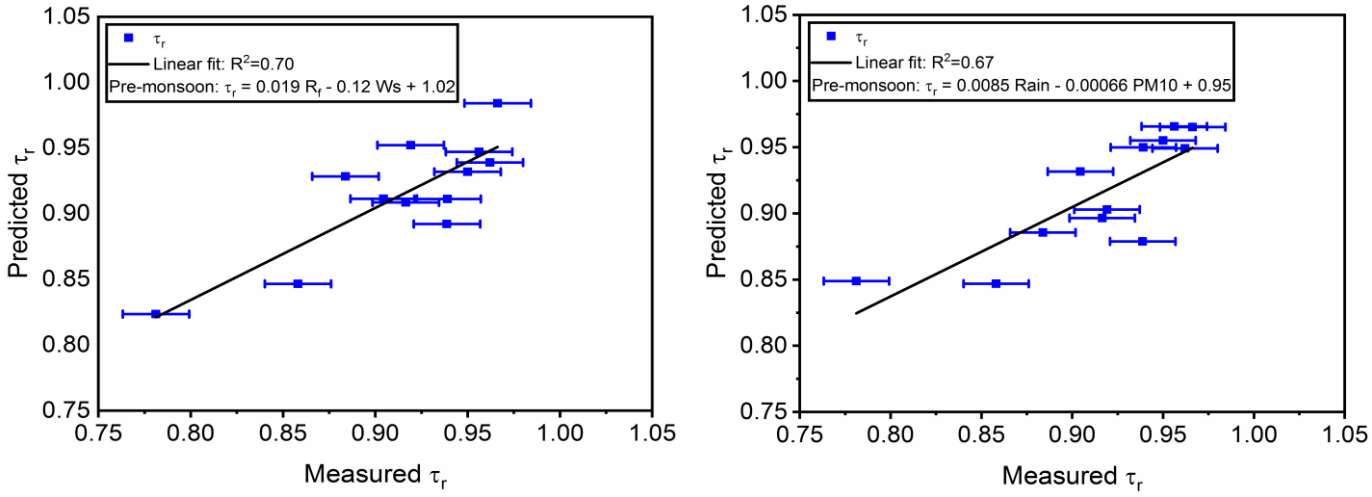

Figure 10. Regression plot of predicted transmittance and measured transmittance of weekly cleaned glass (G2) using the MLR model during pre-monsoon season for various environmental parameters: (**a**) R_f and *Ws* and (**b**) *Rain* and *PM10*. The uncertainty associated with the average relative direct transmittance of the weekly cleaned glass coupon during pre-monsoon is ±0.018.

During the pre-monsoon season (Figure 10), two combinations were found to be significant: (a) R_f and *Ws* (R_f showed a positive correlation and *Ws* showed a negative correlation with τ_r) and (b) *Rain* and *PM10* (*Rain* showed a positive correlation and *PM10* showed a negative correlation). In the first case, an increase in R_f cleans and an increase in *Ws* leads to the soiling of the glass surface. This may be rationalized by considering that frequent rainfall cleans the surface and *Ws* in the range of ≤ 4 m/s tends to deposit dust onto the surface [49]. In the second case, increases in *Rain* and reductions in *PM10* also increase

τ_r (reduces soiling) during the pre-monsoon season. Comparatively speaking, during this season, *PM10* concentration fluctuates the most with the maximum and minimum values of 169.5 µg/m^3 and 50.5 µg/m^3, respectively.

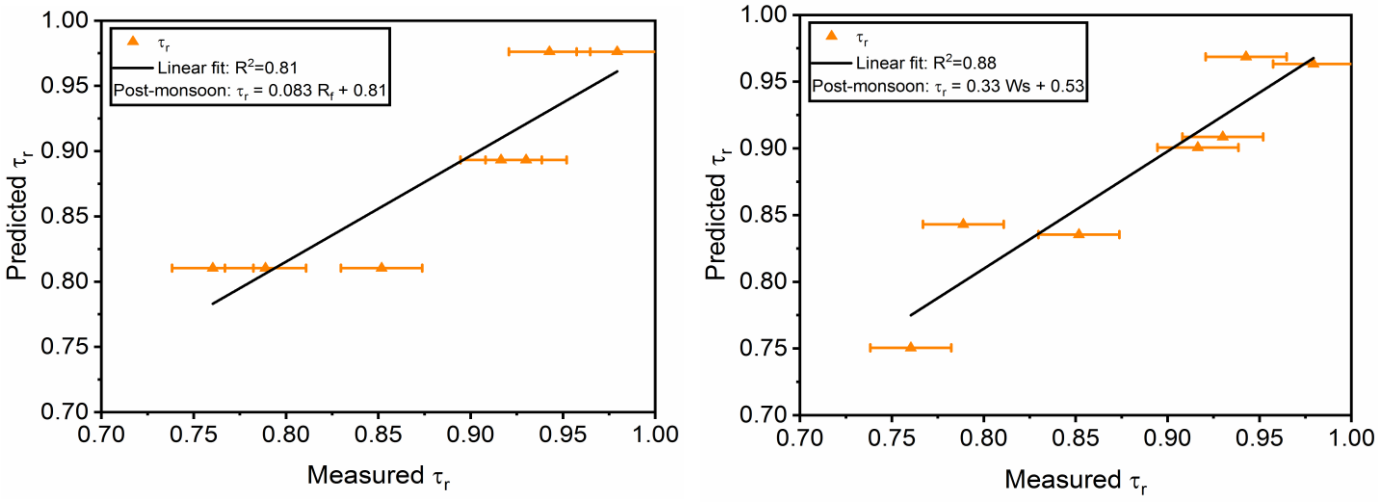

(**a**) (**b**)

Figure 11. Regression plot of predicted transmittance and measured transmittance of weekly cleaned glass (G2) using the MLR model during the post-monsoon season for the environmental parameters: (**a**) R_f and (**b**) *Ws*. The uncertainty associated with the average relative direct transmittance of the weekly cleaned glass coupon during post-monsoon is ±0.022.

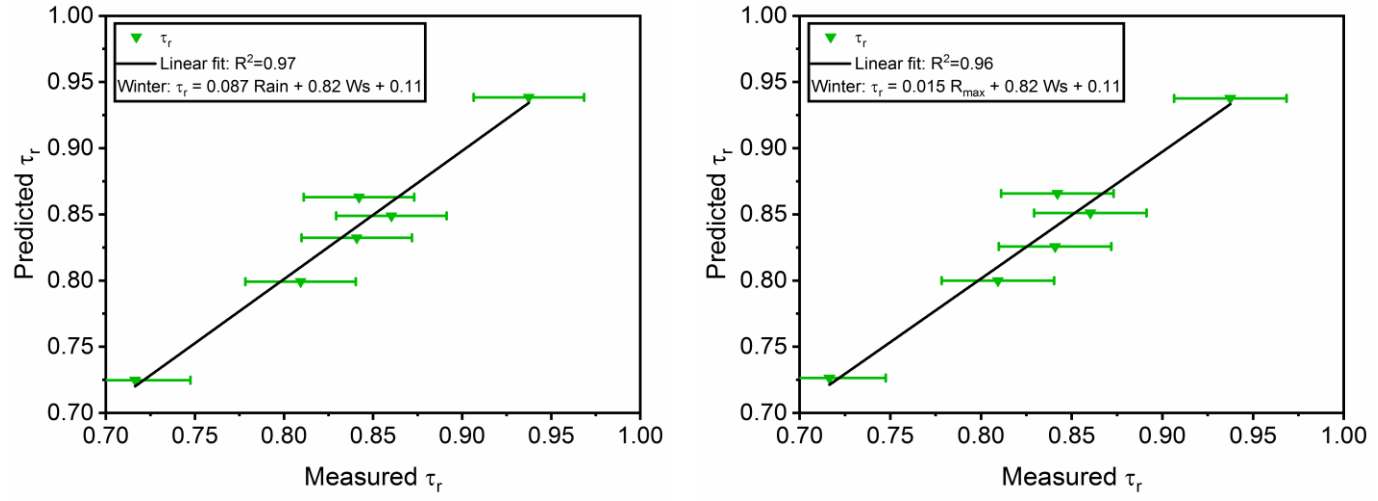

(**a**) (**b**)

Figure 12. Regression plot of predicted transmittance and measured transmittance of weekly cleaned glass (G2) using the MLR model during the winter season for various environmental parameters: (**a**) *Rain* and *Ws* and (**b**) R_{max} and *Ws*. The uncertainty associated with the average relative direct transmittance of the weekly cleaned glass coupon during winter is ±0.031.

The analysis during the post-monsoon season (Figure 11) showed that *Ws* and R_f have a positive correlation with τ_r, but these two parameters affect the transmittance of G2 individually. They do not have interdependency with one another. The *Ws* attributed to cleaning the surface may be because the *Ws* during this season is mostly in the range of 0–2 m/s, which was not sufficient enough to blow the surrounding dust particle to deposit it onto the surface, and lower wind speed leads to less accumulation [50].

During the winter season (Figure 12), we have the following: (a) *Rain* and *Ws* and (b) R_{max} and *Ws* showed a significant correlation. All the environmental parameters in both of the relationships that were determined showed a positive correlation. Increases in both *Rain* and *Ws* simultaneously increased τ_r during the winter season. *Ws* can have two effects on soiling, as reported by Sayyah et al. [48]. During post-monsoon and winter seasons, *Ws* showed a positive correlation, but a negative correlation was observed during pre-monsoon.

No significant relationship between the transmittance and any of the environmental parameters was obtained during the SW monsoon season. Comparably higher *Rain* and R_f during that season lowers the chance of soiling and minimizes the impact of other environmental parameters.

An analysis over the whole year (Figure 13), showed a positive correlation of τ_r with R_f and T_{amb} having a low R^2 value of 0.53; thus, the correlation was not strong. Due to the high seasonality variance of the site under study, the significance of the correlations between the soiling (quantified by the average transmittance) and environmental parameters was highly dependent on the season. Moreover, these correlations are for the considered year of analysis; they may change when more data from two or more years are considered.

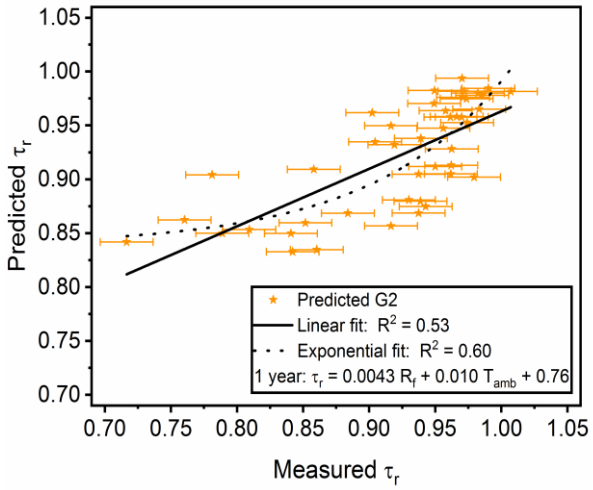

Figure 13. Regression plot of predicted transmittance and measured transmittance of weekly cleaned glass (G2) using the MLR model for a year. The uncertainty associated with the average relative direct transmittance of the weekly cleaned glass coupon is ±0.02. The solid line represents the linear fit and the dashed line represents an exponential fit with an offset to guide the eye. For the values of parameters of the linear and exponential fits refer to Tables S8 and S9.

3.5. Cleaning Cycle and Seasonal Analysis

As part of the comprehensive analysis outlined in Figure 1, the seasonal τ_{loss} of the glass coupons G2, G3, and G4 during various seasons over the year is shown in Figure 14. These average values are also presented in Table 1. The annual average transmittance loss due to soiling was 7.9%, 10%, and 12.9% for weekly (G2), monthly (G3), and never (G4) cleaning cycles, respectively. As discussed in the earlier section for the statistical *t*-test analysis, recommendations are made regarding the cleaning cycle on a seasonal basis. In a location like Tezpur with high *RH*, a warm and wet monsoon season, and a dry winter, weekly cleaning can maintain a high weekly τ_r above 80% during post-monsoon and winter seasons and monthly cleaning can maintain the weekly τ_r above 90% during pre-monsoon and SW monsoon seasons.

To evaluate the potential effect of soiling on PV energy production in the various seasons, the loss in energy generation of PV modules was calculated using Equation (5) on a seasonal and annual basis under standard test conditions (STC). The results are shown in Figure 15 (the electrical specifications of the considered PV panel are tabulated in Table S10); it was found that the annual average E_{loss} due to soiling was 116.6 Wh/m^2/day (7.9%),

147.5 Wh/m^2/day (9.9%), and 190 Wh/m^2/day (12.7%) for weekly (G2), monthly (G3), and never (G4) cleaning cycles, respectively. On a seasonal basis, the E_{loss} observed from high to low was in the order: winter > post-monsoon > pre-monsoon > SW monsoon. (For a detailed weekly E_{loss}, see Figure S10.) In addition, the variation in H_s within each season led to the variation in the overall E_{loss} for a particular season. It could be observed that the τ_{loss} and E_{loss} were almost identical, with a slight difference during high-soiling conditions. As these energy losses are calculated for the ideal conditions (Standard AM1.5D), a complete description should include the actual spectral irradiance distribution for the season. This is because in actual outdoor conditions, the spectral distribution, $E_D(\lambda,t)$ in Equation (10), of the solar irradiance levels will vary, and so too will the E_{loss}.

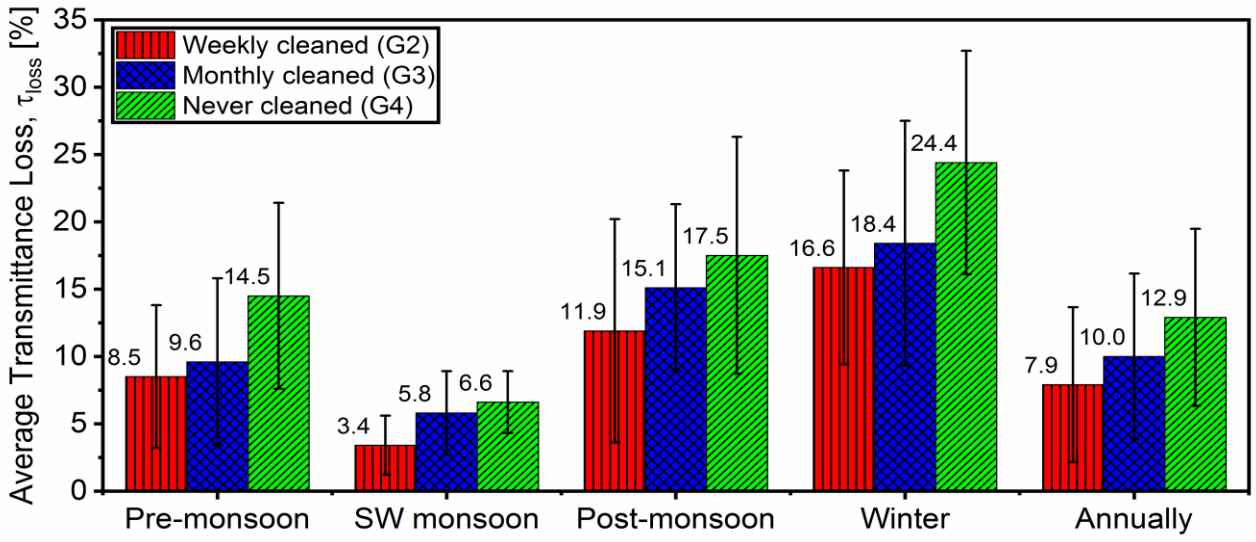

Figure 14. Seasonal average transmittance loss (τ_{loss}) and the respective standard deviation (in %) of weekly cleaned (G2), monthly cleaned (G3), and never cleaned (G4) glass coupons during the four seasons.

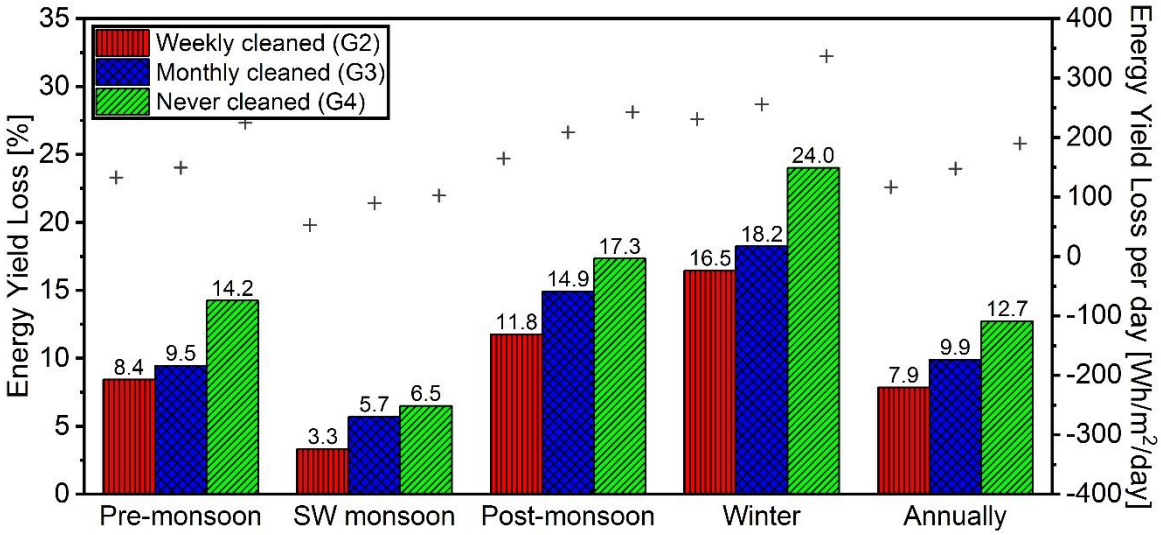

Figure 15. Energy yield loss percentage due to soiling for different cleaning cycles during the four seasons and annually at STC. The "+" symbol denotes the (predicted) energy yield loss in Wh/m^2/day for the right side of the y-axis.

4. Discussion

Our novel method, shown in Figure 1, can be used to evaluate the effectiveness of different cleaning cycles (frequencies) and to explore the seasonality of soiling. It allows for a systematic organization and analysis of fundamental soiling data.

Soiling is a site-specific issue, which can vary from installation to installation. The elemental composition of the soiling experienced at the investigated site is described in the Supplemental Material and has been sourced from previous literature [51–54]. However, there are some general trends that can be learned from this study, as well as some recommendations for improvements in subsequent studies. For example, for the whole year, more frequent cleaning cycles tend to result in lower transmittance losses, while less frequent cleaning cycles are not as effective. Although somewhat intuitive, this is not the case for some weeks. The reason is the non-uniform distribution of the soiling [55,56]. This non-uniformity generates high uncertainty, especially during seasons with high-soiling conditions (winter and post-monsoon). Future studies should therefore consider multiple transmittance measurements per coupon, and more coupons, to minimize the uncertainty in relative direct transmittance.

For the statistical F-test and *t*-test analysis, since our data do not have replicates for the coupons, there is also some uncertainty. Two average values (means) that are statistically different or statistically the same might not always be that way. This can be due to the high standard deviation and uncertainty in the measurements [57], which are in part caused by the non-uniformity of the soiling and the nature of the soiling itself. Our results suggest that more replicates of glass coupons with similar cleaning cycles need to be exposed outdoors to reduce measurement errors (for example, from stochastic events). Still, our methodology, emphasizing the use of simple and reliable F- and *t*-test statistics can be employed for a variety of conditions at sites worldwide to recommend likely best practices for cleaning strategies. There exist some other statistical techniques, such as MANOVA and MANCOVA, that could also be used in future work with the possibility to achieve better results.

Our results suggest that water (in the form of rain or dew) does not provide a complete cleaning method. Dew can act as both a cleaning agent and a soiling agent. For a tilted surface, as the surface approaches the dew point temperature, T_d, it may have a cleaning effect. In the present study, it may not have had a cleaning effect since the glass coupons were placed horizontally. Therefore, for both rain and dew, results may be different for glass (or PV modules) that are tilted (10°, 30°, 45°, 60°, and 90°). Future studies can include this topic.

A preliminary correlation between soiling loss (in terms of average relative direct transmittance) and a few environmental parameters, for the site under study, was determined using the linear regression models (SLR and MLR). Our methodology shows that with high seasonality for a site, even the significance of correlations between the transmittance and environmental parameters changes with each season. Some parameters that show significance during one season may not have any significance in a different season. Soiling loss is very much dependent on the season and even the impact of the dominant environmental parameters changes with each season. Therefore, it may not be possible to develop a universal or general correlation of soiling losses with all the environmental parameters over the year.

The methodology allows for the study of the seasonality of the correlations between soiling (in terms of transmittance) and the environmental parameters for a given location. The results reported in this work can not only significantly benefit the PV deployment and maintenance in the region of study, but the results are also applicable to many additional locations with similar environmental conditions. It may not be applicable throughout the entire year, but the results, and certainly the methodology, can be applied for a specific season of the year at another location. The general results can likely be applied to other areas with a Köppen–Geiger [27] Cwa climate classification; that is, a humid subtropical climate with a dry winter. This would require further tests and validation.

5. Conclusions

A novel method has been utilized to analyze the difference in the net soiling for different cleaning cycles during seasons exhibiting a variety of environmental conditions. Such methods can be beneficial to establish best practices for the cleaning strategy of PV modules for diverse conditions worldwide. The transmittance loss (τ_{loss}) due to the soiling of horizontally mounted glass coupons installed at a humid subtropical location with a dry winter was found to be (in order from high to low): winter > post-monsoon > pre-monsoon > SW monsoon seasons. Based on the statistical (F- and *t*-test) analysis, the present study recommends weekly cleaning during winter and post-monsoon to maintain high transmittance above 80%, as well as an optimal cleaning cycle of once a month during the pre-monsoon and SW monsoon seasons to maintain high transmittance above 90%. It was observed that rain was not a complete or sufficient way of cleaning; a minimum rainfall threshold is required, depending on the cleaning strategy. The threshold rainfall required to clean the weekly cleaned glass coupon, was the highest, followed by that of the monthly and never cleaned glass coupons. Linear regression analysis suggests that environmental parameters which show significance during one season do not necessarily have a strong correlation to soiling in another season. It may thus prove difficult to develop a simple empirical relationship for soiling losses. In general, the findings of this study demonstrate the usefulness of statistical analysis of experimental data in outdoor conditions to elucidate the effect of environmental factors and seasonality on the soiling of solar energy conversion systems.

Supplementary Materials: The following supporting information can be downloaded at: https://www.mdpi.com/article/10.3390/en15240000/s1, Figure S1: EDS analysis; Figure S2: FESEM analysis; Table S1: Elemental composition in weight percentage of dust outdoor from EDS analysis; Figure S3: Rose diagram of wind direction; Table S2: Distribution of wind speed for various seasons; Figure S4: Direct relative transmittance data fit to the modified Ångström turbidity equation for glass coupon; Figure S5: The average relative direct transmittance versus offset parameter of Ångström turbidity equation; Figure S6: *t*-test *p*-value of the combination of seasons for various glass coupons; Table S3: Parameter value from the logistic fit for the average relative direct transmittance versus weekly maximum rainfall; Figure S7: Correlation between the average relative direct transmittance, average weekly PM10 and relative humidity; Figure S8: Relation between the average relative direct transmittance, average weekly PM10 (a) average weekly ΔT and (b) dew point temperature; Table S4: Parameter value from linear fit for the average relative direct transmittance versus average air temperature; Table S5: Parameter value from linear fit for the average relative direct transmittance versus average dew point temperature; Table S6: The correlation between average relative direct transmittance and environmental parameters obtained using SLR model; Table S7: The correlation between the measured and predicted average relative direct transmittance obtained using MLR models; Table S8: Parameter value for the linear fit for the annual analysis using MLR model. Table S9: Parameter value for the exponential fit for the annual analysis using MLR model; Table S10: Electrical data of the PV module; Figure S9: External quantum efficiency and spectral response of monocrystalline solar cell; Figure S10: Weekly energy yield loss at standard test conditions.

Author Contributions: Conceptualization, H.B., L.M., G.P.S. and N.S.; methodology, H.B., S.P., L.M., G.P.S. and N.S.; software, H.B.; validation, H.B., L.M., G.P.S. and N.S.; formal analysis, H.B.; investigation, H.B., S.P., L.M., G.P.S. and N.S.; data curation, H.B., S.P. and N.S.; writing—original draft preparation, H.B.; writing—review and editing, H.B., L.M., G.P.S. and N.S. All authors have read and agreed to the published version of the manuscript.

Funding: Honey Brahma acknowledges the Ministry of Tribal Affairs, India, for providing a Ph.D. Fellowship National Fellowship for Higher Education for ST students 2017-18. The authors also acknowledge the support received from the project 'India-UK Center for Education and Research in Clean Energy' (DST/RCUK/JVCCE/2015/04 (G) dated 27 February 2017) during this research work. The work of Leonardo Micheli is supported by Sole4PV, a project funded by the Italian Ministry of University and Research under the 2019 «Rita Levi Montalcini» Program for Young Researchers.

Data Availability Statement: Not applicable.

Acknowledgments: The authors are grateful to Pranab Mudoi, Department of MBBT, Tezpur University and IIT Guwahati for the technical assistance, as well as general support from the Solar Radiation Resource Assessment of India (SRRA) project and Pollution Control Board, Department of Environment and Forest, Assam.

Conflicts of Interest: The authors declare no conflict of interest.

References

1. International Energy Agency; International Renewable Energy Agency; United Nations Statistics Division; World Bank; World Health Organization. *Tracking SDG 7: The Energy Progress Report 2021*; World Bank: Washington, DC, USA, 2021.
2. International Energy Agency. *Task 1 Strategic PV Analysis and Outreach-2020 Snapshot of Global PV Markets*; International Energy Agency: Paris, France, 2021.
3. Ali, A.; Irshad, K.; Khan, M.F.; Hossain, M.M.; Al-Duais, I.N.; Malik, M.Z. Artificial intelligence and bio-inspired soft computing-based maximum power plant tracking for a solar photovoltaic system under non-uniform solar irradiance shading conditions—A review. *Sustainability* **2021**, *13*, 10575. [CrossRef]
4. Maghami, M.R.; Hizam, H.; Gomes, C.; Radzi, M.A.; Rezadad, M.I.; Hajighorbani, S. Power loss due to soiling on solar panel: A review. *Renew. Sustain. Energy Rev.* **2016**, *59*, 1307–1316. [CrossRef]
5. Laarabi, B.; El Baqqal, Y.; Dahrouch, A.; Barhdadi, A. Deep analysis of soiling effect on glass transmittance of PV modules in seven sites in Morocco. *Energy* **2020**, *213*, 118811. [CrossRef]
6. El-Nashar, A.M. The effect of dust accumulation on the performance of evacuated tube collectors. *Sol. Energy* **1994**, *53*, 105–115. [CrossRef]
7. Chanchangi, Y.N.; Ghosh, A.; Baig, H.; Sundaram, S.; Mallick, T.K. Soiling on PV performance influenced by weather parameters in Northern Nigeria. *Renew. Energy* **2021**, *180*, 874–892. [CrossRef]
8. Olivares, D.; Ferrada, P.; Bijman, J.; Rodríguez, S.; Trigo-González, M.; Marzo, A.; Rabanal-Arabach, J.; Alonso-Montesinos, J.; Batlles, F.J.; Fuentealba, E. Determination of the soiling impact on photovoltaic modules at the coastal area of the Atacama Desert. *Energies* **2020**, *13*, 3819. [CrossRef]
9. Al Shehri, A.; Parrott, B.; Carrasco, P.; Al Saiari, H.; Taie, I. Impact of dust deposition and brush-based dry cleaning on glass transmittance for PV modules applications. *Sol. Energy* **2016**, *135*, 317–324. [CrossRef]
10. Boyle, L.; Flinchpaugh, H.; Hannigan, M. Natural soiling of photovoltaic cover plates and the impact on transmission. *Renew. Energy* **2015**, *77*, 166–173. [CrossRef]
11. Mithhu, M.M.H.; Rima, T.A.; Khan, M.R. Global analysis of optimal cleaning cycle and profit of soiling affected solar panels. *Appl. Energy* **2021**, *285*, 116436. [CrossRef]
12. Yadav, S.K.; Kumar, N.M.; Ghosh, A.; Bajpai, U.; Chopra, S.S. Assessment of soiling impacts and cleaning frequencies of a rooftop BAPV system in composite climates of India. *Sol. Energy* **2022**, *242*, 119–129. [CrossRef]
13. Picotti, G.; Borghesani, P.; Cholette, M.; Manzolini, G. Soiling of solar collectors—Modelling approaches for airborne dust and its interactions with surfaces. *Renew. Sustain. Energy Rev.* **2018**, *81*, 2343–2357. [CrossRef]
14. Costa, S.C.; Diniz, A.S.A.; Kazmerski, L.L. Solar energy dust and soiling R&D progress: Literature review update for 2016. *Renew. Sustain. Energy Rev.* **2018**, *82*, 2504–2536.
15. Khan, M.A.; Islam, N.; Khan, M.A.M.; Irshad, K.; Hanzala, M.; Pasha, A.A.; Mursaleen, M. Experimental and simulation analysis of grid-connected rooftop photovoltaic system for a large-scale facility. *Sustain. Energy Technol. Assess.* **2022**, *53*, 102773. [CrossRef]
16. Micheli, L.; Deceglie, M.G. *Predicting Future Soiling Losses Using Environmental Data*; National Renewable Energy Laboratory (NREL): Golden, CO, USA, 2018.
17. Figgis, B.; Ennaoui, A.; Guo, B.; Javed, W.; Chen, E. Outdoor soiling microscope for measuring particle deposition and resuspension. *Sol. Energy* **2016**, *137*, 158–164. [CrossRef]
18. El-Nashar, A.M. Effect of dust deposition on the performance of a solar desalination plant operating in an arid desert area. *Sol. Energy* **2003**, *75*, 421–431. [CrossRef]
19. Tanesab, J.; Parlevliet, D.; Whale, J.; Urmee, T. Seasonal effect of dust on the degradation of PV modules performance deployed in different climate areas. *Renew. Energy* **2017**, *111*, 105–115. [CrossRef]
20. Javed, W.; Guo, B.; Figgis, B.; Pomares, L.M.; Aïssa, B. Multi-year field assessment of seasonal variability of photovoltaic soiling and environmental factors in a desert environment. *Sol. Energy* **2020**, *211*, 1392–1402. [CrossRef]
21. Coello, M.; Boyle, L. Simple Model For Predicting Time Series Soiling of Photovoltaic Panels. *IEEE J. Photovolt.* **2019**, *9*, 1382–1387. [CrossRef]
22. Javed, W.; Guo, B.; Figgis, B. Modeling of photovoltaic soiling loss as a function of environmental variables. *Sol. Energy* **2017**, *157*, 397–407. [CrossRef]
23. Hossain, M.I.; Ali, A.; Bermudez Benito, V.; Figgis, B.; Aïssa, B. Anti-Soiling Coatings for Enhancement of PV Panel Performance in Desert Environment: A Critical Review and Market Overview. *Materials* **2022**, *15*, 7139. [CrossRef]
24. Abraim, M.; Salihi, M.; El Alani, O.; Hanrieder, N.; Ghennioui, H.; Ghennioui, A.; El Ydrissi, M.; Azouzoute, A. Techno-economic assessment of soiling losses in CSP and PV solar power plants: A case study for the semi-arid climate of Morocco. *Energy Convers. Manag.* **2022**, *270*, 116285. [CrossRef]

25. Abdallah, R.; Juaidi, A.; Abdel-Fattah, S.; Qadi, M.; Shadid, M.; Albatayneh, A.; Çamur, H.; García-Cruz, A.; Manzano-Agugliaro, F. The Effects of Soiling and Frequency of Optimal Cleaning of PV Panels in Palestine. *Energies* **2022**, *15*, 4232. [CrossRef]
26. Kimber, A.; Mitchell, L.; Nogradi, S.; Wenger, H. The effect of soiling on large grid-connected photovoltaic systems in California and the southwest region of the United States. In Proceedings of the 2006 IEEE 4th World Conference on Photovoltaic Energy Conference, Waikoloa, HI, USA, 7–12 May 2006; IEEE: New York, NY, USA, 2006; pp. 2391–2395.
27. Kottek, M.; Grieser, J.; Beck, C.; Rudolf, B.; Rubel, F. World map of the Köppen-Geiger climate classification updated. *Meteorol. Z.* **2006**, *15*, 259–263. [CrossRef]
28. Rao, Y.P. The climate of the Indian subcontinent. In *World Survey of Climatology*; Takahasi, K., Arakawa, H., Eds.; Elsevier: Amsterdam, The Netherlands, 1981; Volume 9, pp. 67–182.
29. Jain, S.; Kumar, V.; Saharia, M. Analysis of rainfall and temperature trends in northeast India. *Int. J. Climatol.* **2013**, *33*, 968–978. [CrossRef]
30. Ilse, K.; Figgis, B.; Khan, M.Z.; Naumann, V.; Hagendorf, C. Dew as a detrimental influencing factor for soiling of PV modules. *IEEE J. Photovolt.* **2018**, *9*, 287–294. [CrossRef]
31. Figgis, B.; Nouviaire, A.; Wubulikasimu, Y.; Javed, W.; Guo, B.; Ait-Mokhtar, A.; Belarbi, R.; Ahzi, S.; Rémond, Y.; Ennaoui, A. Investigation of factors affecting condensation on soiled PV modules. *Sol. Energy* **2018**, *159*, 488–500. [CrossRef]
32. Garg, H. Effect of dirt on transparent covers in flat-plate solar energy collectors. *Sol. Energy* **1974**, *15*, 299–302. [CrossRef]
33. Smestad, G.P.; Germer, T.A.; Alrashidi, H.; Fernández, E.F.; Dey, S.; Brahma, H.; Sarmah, N.; Ghosh, A.; Sellami, N.; Hassan, I.A.; et al. Modelling photovoltaic soiling losses through optical characterization. *Sci. Rep.* **2020**, *10*, 58. [CrossRef]
34. Burton, P.D.; Boyle, L.; Griego, J.J.; King, B.H. Quantification of a minimum detectable soiling level to affect photovoltaic devices by natural and simulated soils. *IEEE J. Photovolt.* **2015**, *5*, 1143–1149. [CrossRef]
35. Boyle, L.; Flinchpaugh, H.; Hannigan, M. Assessment of PM dry deposition on solar energy harvesting systems: Measurement–model comparison. *Aerosol Sci. Technol.* **2016**, *50*, 380–391. [CrossRef]
36. Conceicao, R.; Silva, H.G.; Mirao, J.; Gostein, M.; Fialho, L.; Narvarte, L.; Collares-Pereira, M. Saharan dust transport to Europe and its impact on photovoltaic performance: A case study of soiling in Portugal. *Sol. Energy* **2018**, *160*, 94–102. [CrossRef]
37. Nayshevsky, I.; Xu, Q.; Lyons, A.M. Hydrophobic–hydrophilic surfaces exhibiting dropwise condensation for anti-soiling applications. *IEEE J. Photovolt.* **2018**, *9*, 302–307. [CrossRef]
38. Korevaar, M.; Mes, J.; Merrouni, A.A.; Bergmans, T.; Van Mechelen, X. Unique Soiling Detection System for PV Modules. In Proceedings of the 35th European PV Solar Energy Conference and Exhibition, Brussels, Belgium, 24–28 September 2018; p. 1988e90.
39. Aïssa, B.; Scabbia, G.; Figgis, B.W.; Lopez, J.G.; Benito, V.B. PV-soiling field-assessment of Mars™ optical sensor operating in the harsh desert environment of the state of Qatar. *Sol. Energy* **2022**, *239*, 139–146. [CrossRef]
40. World Meteorological Organisation. *Commission for Instruments and Methods of Observation (CIMO-VIII)*, 8th ed.; World Meteorological Organisation, Ed.; Secretariat of the World Meteorological Organisation: Geneva, Switzerland, 1982.
41. *IEC 61724-1*; Photovoltaic system performance—Part 1: Monitoring; Edition 1.0, 2017–03. International Electrotechnical Commission: Geneva, Switzerland, 2017.
42. Fernández-Solas, Á.; Micheli, L.; Almonacid, F.; Fernández, E.F. Indoor validation of a multiwavelength measurement approach to estimate soiling losses in photovoltaic modules. *Sol. Energy* **2022**, *241*, 584–591. [CrossRef]
43. *ASTM-G173-03*; Standard Tables for Reference Solar Spectral Irradiances: Direct Normal and Hemispherical on 37° Tilted Surface. ASTM International: West Conshohocken, PA, USA, 2003.
44. Mangiafico, S.S. *Summary and Analysis of Extension Program Evaluation in R*; Rutgers Cooperative Extension: New Brunswick, NJ, USA, 2016.
45. Saud, S.; Jamil, B.; Upadhyay, Y.; Irshad, K. Performance improvement of empirical models for estimation of global solar radiation in India: A k-fold cross-validation approach. *Sustain. Energy Technol. Assess.* **2020**, *40*, 100768. [CrossRef]
46. Isaifan, R.J.; Johnson, D.; Ackermann, L.; Figgis, B.; Ayoub, M. Evaluation of the adhesion forces between dust particles and photovoltaic module surfaces. *Sol. Energy Mater. Sol. Cells* **2019**, *191*, 413–421. [CrossRef]
47. Micheli, L.; Deceglie, M.G.; Muller, M. Predicting photovoltaic soiling losses using environmental parameters: An update. *Prog. Photovolt. Res. Appl.* **2019**, *27*, 210–219. [CrossRef]
48. Sayyah, A.; Horenstein, M.N.; Mazumder, M.K. Energy yield loss caused by dust deposition on photovoltaic panels. *Sol. Energy* **2014**, *107*, 576–604. [CrossRef]
49. Mani, M.; Pillai, R. Impact of dust on solar photovoltaic (PV) performance: Research status, challenges and recommendations. *Renew. Sustain. Energy Rev.* **2010**, *14*, 3124–3131. [CrossRef]
50. Goossens, D.; Van Kerschaever, E. Aeolian dust deposition on photovoltaic solar cells: The effects of wind velocity and airborne dust concentration on cell performance. *Sol. Energy* **1999**, *66*, 277–289. [CrossRef]
51. Ministry of Mines. Minerals blocks on auction in 2018-19. In *4th National Conclave on Mines and Minerals 2018*; Government of Assam: Indore, India, 2018.
52. Indian Bureau of Mines. *Indian Minerals Yearbook 2015 (Part I) State Reviews (Assam)*, 54th ed.; Ministry of Mines, G.o.I., Ed.; Indian Bureau of Mines: Nagpur, India, 2017.
53. Khare, P.; Baruah, B.P. Elemental characterization and source identification of PM2.5 using multivariate analysis at the suburban site of North-East India. *Atmos. Res.* **2010**, *98*, 148–162. [CrossRef]

54. Bhuyan, P.; Deka, P.; Prakash, A.; Balachandran, S.; Hoque, R.R. Chemical characterization and source apportionment of aerosol over mid Brahmaputra Valley, India. *Environ. Pollut.* **2018**, *234*, 997–1010. [CrossRef] [PubMed]
55. Said, S.A.; Walwil, H.M. Fundamental studies on dust fouling effects on PV module performance. *Solar Energy* **2014**, *107*, 328–337. [CrossRef]
56. El-Shobokshy, M.; Mujahid, A.; Zakzouk, A. Effects of dust on the performance of concentrator photovoltaic cells. *IEE Proc. I (Solid-State Electron Devices)* **1985**, *132*, 5–8. [CrossRef]
57. Meyer, V.R. Measurement uncertainty. *J. Chromatogr. A* **2007**, *1158*, 15–24. [CrossRef] [PubMed]